

## RESEARCH ARTICLE



WILEY

# New library of pyrazole–imidazo[1,2- $\alpha$ ]pyridine molecular conjugates: Synthesis, antibacterial activity and molecular docking studies

 Oluwakemi Ebenezer  | Paul Awolade | Neil Koorbanally | Parvesh Singh

School of Chemistry, University of KwaZulu-Natal, Durban, South Africa

## Correspondence

Neil Koorbanally and Parvesh Singh, School of Chemistry and Physics, University of KwaZulu-Natal, P/Bag X54001, Westville, Durban, South Africa-4000.

Email: singhp4@ukzn.ac.za, parveshdurban@gmail.com (P.S.), koorbanally@ukzn.ac.za (N.K)

## Funding information

National Research Foundation South Africa for a Competitive Grant for Rated Researchers, Grant/Award Number: 118534; Incentive Funding for Rated Researchers, Grant/Award Number: 114817

## Abstract

A library of novel pyrazole–imidazo[1,2- $\alpha$ ]pyridine scaffolds was designed and synthesized through a one-pot three-component tandem reaction. The structures of synthesized conjugates were confirmed by spectroscopic techniques (NMR, IR and HRMS). In vitro antibacterial evaluation of the twelve synthesized molecules (**7a**, **8a–k**) against methicillin-resistant *Staphylococcus aureus* and normal strains of *Escherichia coli*, *Salmonella typhimurium*, *Klebsiella pneumonia* and *Pseudomonas aeruginosa* established **8b**, **8d**, **8e**, **8h** and **8i** as potent antibacterial agents with superior minimum bactericidal concentration, compared with standard drug ciprofloxacin. Molecular docking studies of all active compounds into the binding site of glucosamine-6-phosphate synthase were further performed in order to have a comprehensive understanding of putative binding modes within the active sites of the receptor.

## KEYWORDS

 antibacterial, imidazo[1,2- $\alpha$ ]pyridine, molecular docking, pyrazole, tandem reaction

## 1 | INTRODUCTION

Bacterial infections still pose a huge threat to smooth and efficient clinical practice due to the recent loss in potency of current antibacterial agents precipitated by increased antimicrobial resistance. Thus, the global emergence of multidrug-resistant (MDR) bacteria is one of the greatest challenges in public health care. Each year in the United States, at least 2 million people get an antibiotic-resistant infection and at least 23,000 people die ([www.cdc.gov/drugresistance/index.html](http://www.cdc.gov/drugresistance/index.html)).

MDR bacteria are particularly threatening, since they are resistant to virtually all available antibiotics. Currently, there is a wide repertoire of available antibacterial agents, the most popular being the penicillins and fluoroquinolones (Pannu & Nadim, 2008). However, the serious side-effects of currently available antibacterial drugs cannot be neglected, which includes multi-system processes characterized by high blood pressure and life-threatening skin rashes, such as erythema multiforme and toxic epidermal necrolysis. Other

notable side-effects are neuropathy, nephrotoxicity, ototoxicity, hepatotoxicity and bone marrow diseases (Bagdi, Sougata, Kamarul, & Alakananda, 2015; Finn et al., 2003; Pandit, Mahesh, Yashwant, Nitin, & Vijay, 2018). For instance, though it shares similar potency with penicillin, sulfaphenazole a pyrazole derivative belonging to the sulfonamide class of antibacterial drugs has limited clinical utility due to its toxicity and inherent side-effects. Therefore, despite the growing list of antibacterial agents, an urgent and sustainable effort is needed to produce new antibiotics with improved toxicity profile to counteract the problem of antibiotic resistance.

Several approaches have been employed for the development of new and efficient antibacterial agents that can overcome resistance. Molecular hybridization emerges as one of the best approaches to obtain novel molecular assemblies as efficient antibacterial agent. The strategy involves merging two or more bioactive pharmacophores into a single molecular scaffold, in the hope of the new hybrid drug having

better efficacy than the parent molecules and with minimal side-effects (Gueffier & Gueffier, 2007; Pandit et al., 2018). Hybridization of antibacterial agent can reduce the occurrence of resistant mutations, particularly, when resistance is higher in one of the antibacterial components (Xi et al., 2017).

Pyrazoles are one of the most important classes of five-membered heterocyclic compounds, which are scarcely found in nature apparently due to difficulty in the formation of N–N bond by living organisms. Pyrazole-based compounds have displayed diverse biological properties such as anti-inflammatory (Yang et al., 2017), antiprotozoal (Hayakawa et al., 2007), antiviral (Márquez-Flores, Campos-Aldrete, Salgado-Zamora, Correa-Basurto, & Meléndez-Camargo, 2012), antifungal (Rao, Barnali, Ranjit, & Kaushik, 2018) and antibacterial activities (Hiremathad et al., 2015; Palanisamy, Samson, Packianathan, & Sudalaiandi, 2013). For example, pyrazole derivatives were found to significantly improve the potency on bacterial methionyl-tRNA synthetase and selectivity over human methionyl-tRNA synthetase (Tomi, Ali, Ahmed, & Mohammed, 2016). Similarly, imidazo[1,2- $\alpha$ ]pyridine has been identified as a promising scaffold and a druggable moiety due to its unavoidable occurrence in numerous clinical drugs, such as zolpidem, saripidem, olprinone, zolimidine, rifaximin and antimycobacterium tuberculosis drug candidates ND-09759 and Q203 currently in clinical trials (Jayanna, Vagdevi, Dharshan, Raghavendra, & Sandeep, 2013; Khan et al., 2017). Compounds containing Imidazo[1,2- $\alpha$ ]pyridine have also been described to possess good anticancer (Daina, Olivier, & Vincent, 2017; Guchhait, Ajay, & Garima, 2012; Milewski, 2002; Montero-Morán, Lara-González, Alvarez-Añorve, Plumbridge, & Calcagno, 2001), antiviral (Ertl, Bernhard, & Paul, 2000), anti-inflammatory (Beadle & Shoichet, 2002) and antibacterial (Al-Tel & Al-Qawasmeh, 2010) activities.

Among the various targets of pyrazole and imidazo[1,2- $\alpha$ ]pyridine, L-glutamine:D-fructose-6-phosphate amidotransferase (GlcN-6-P synthase; EC 2.6.1.16), the sole member of the aminotransferase sub-family of enzymes (Jayanna et al., 2013; Khan et al., 2017; Tomi et al., 2016), which catalyses the formation of glucosamine-6-phosphate from glutamine through fructosamine-6-phosphate, plays an essential role in the cell wall assembly for micro-organisms and human cell (Montero-Morán et al., 2001). GlcN-6-P synthase also regulates enzyme for the pathway leading to the formation of UDP-N-acetylglucosamine (Daina et al., 2017; Tsuiki & Miyagi, 1977). The short-time inactivation of GlcN-6-P synthase is harmful to the pathogenic micro-organism by inducing morphological changes, agglutination and lysis (Chmara & Borowski, 1986) and, hence, making the enzyme a potential target for antibacterial agents development (Barreteau et al., 2008; Ebrahimipour et al., 2016; Ebrahimipour, Mehrji, Jonathan, & Sahar, 2018; Khan et al., 2017; Kumara,

Suhas, Suyoga, Shobha, & Channe, 2018; Sarojini, Krishna, Darshanraj, Bharath, & Manjunatha, 2010).

Here, we report the synthesis of new pyrazole–imidazo[1,2- $\alpha$ ]pyridine hybrids with promising potentials to be good antibacterial agents. To the best of our knowledge, this is the first report on the synthesis and antibacterial activity of pyrazole–imidazo[1,2- $\alpha$ ]pyridine hybrids. Molecular docking study was further employed to gain better insight into the hybrids' potency whilst attempting to provide a mechanism for the action of compounds as inhibitors of GlcN-6-P synthase.

## 2 | METHODS AND MATERIALS

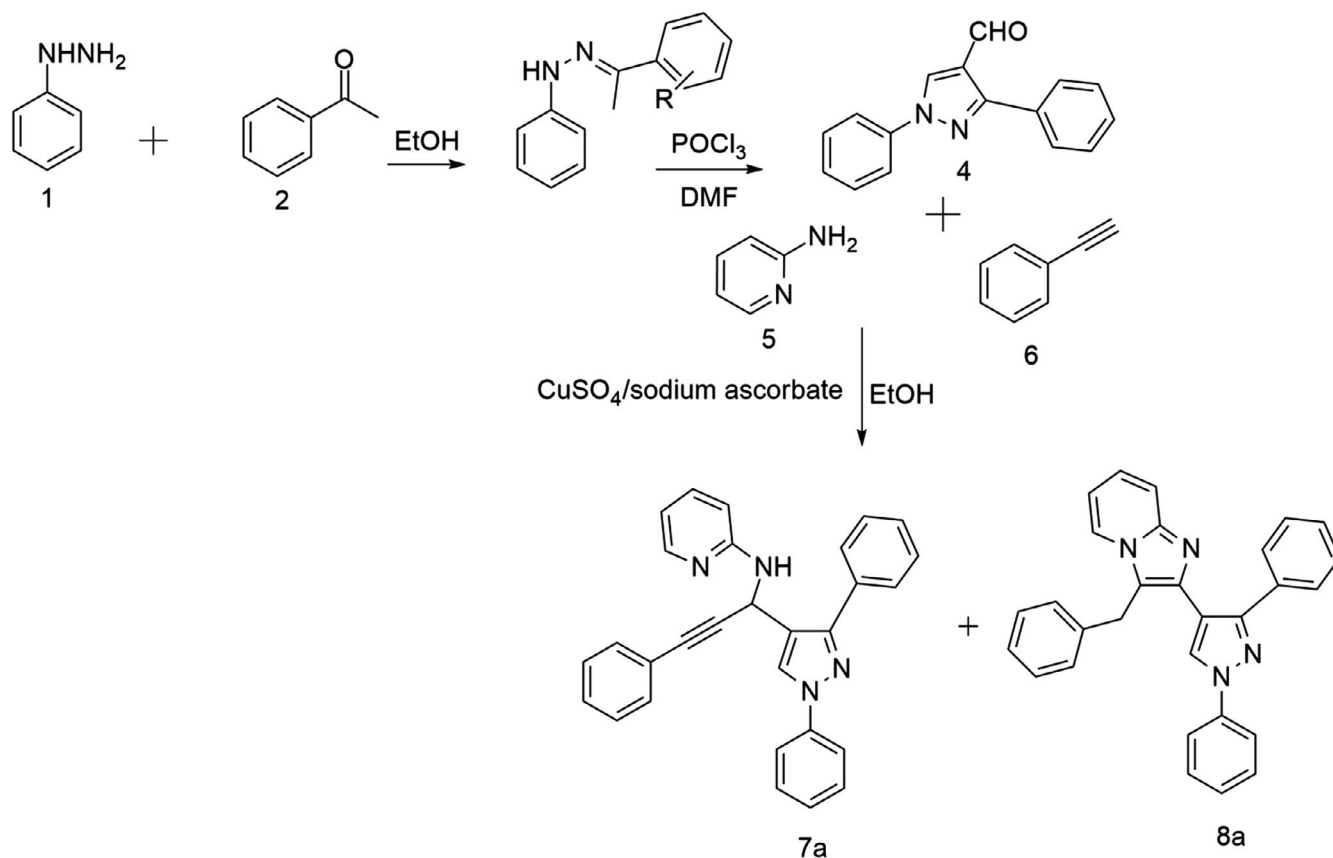
### 2.1 | Chemistry

Reagent grade chemicals were purchased from Sigma-Aldrich, South Africa. Infrared (IR) spectra were recorded on a Perkin Elmer Spectrum 100 FT-IR spectrometer with a Universal ATR sampling accessory.  $^1\text{H}$  and  $^{13}\text{C}$  NMR spectra were recorded at 298 K with 5–10 mg samples dissolved in 0.5 ml deuterated DMSO in 5 mm NMR tubes using Bruker Avance III 400 and 600 MHz NMR spectrometers. Chemical shifts ( $\delta$ ) are reported in parts per million (ppm) and coupling constants ( $J$ ) in hertz. The  $^1\text{H}$  and  $^{13}\text{C}$  chemical shifts of DMSO- $d_6$  were 2.50 ( $^1\text{H}$ ) and 39.51 ( $^{13}\text{C}$ ), respectively, referenced to the internal standard, TMS. All data were processed and analysed using Bruker Topspin 3.5 software.

### 2.2 | Pharmacological screening

Bacterial cultures were grown in nutrient broth for 24 hr at 37°C and diluted (with broth [Mueller-Hinton]) to  $1.5 \times 10^8$  CFU  $\text{ml}^{-1}$  (0.5 McFarland). The sterile Mueller-Hinton agar (MHA) was poured into sterile Petri dishes (90 mm in diameter), and the medium was allowed to solidify. The diluted bacterial strains were then lawn inoculated onto the plates using a cotton swab. Antibiotic assay discs (6 mm; Whatman, UK) were placed onto the MHA plate that was divided into three equivalent lobes. A 1.0 mg/ml sample of each compound in DMSO was prepared and a 10  $\mu\text{l}$  aliquot placed onto the discs. The plates were then incubated for 18 hr at 37°C. After incubation, all plates were examined for the zone of growth inhibition, and the diameters of these zones were measured in millimetres. Ciprofloxacin (1.0 mg/ml) was used as a positive control.

Compounds having a zone of inhibition >9 mm for all strains were selected as active compounds and evaluated for their minimum bactericidal concentration (MBC) using the broth dilution method, where compounds were dissolved in DMSO (1 mg/ml) and subjected to 50% serial dilution in 1-ml Eppendorf tubes with Mueller-Hinton broth, inoculated with Gram-negative and Gram-positive bacterial cultures



**SCHEME 1** Synthesis of pyrazole Imidazo[1,2- $\alpha$ ]pyridines derivatives

(20  $\mu\text{l}$ ) and then incubated at 37°C for 18 hr. The MBC was recorded as the lowest concentration of an antibacterial agent where no growth of the bacteria was observed.

### 2.3 | Computational studies

The crystal structure of glucosamine-6-phosphate synthase (PDB code: 1JXA) was retrieved from the protein data bank with its ligand, and the active site found around the ligand by using discovery studio visualizer. The 3D structures of all the biologically active compounds were built on ChemSketch. The structures of all active molecules were minimized and converted to pdbqt format by OpenBabel in PyRx 0.8 as ligand for molecular docking. The docking procedure was followed using the standard autodock vina implemented in PyRx. The ligand-protein complex was analysed for interactions, and the 3D pose of most active compounds was taken using Discovery Studio visualizer.

## 3 | RESULT AND DISCUSSION

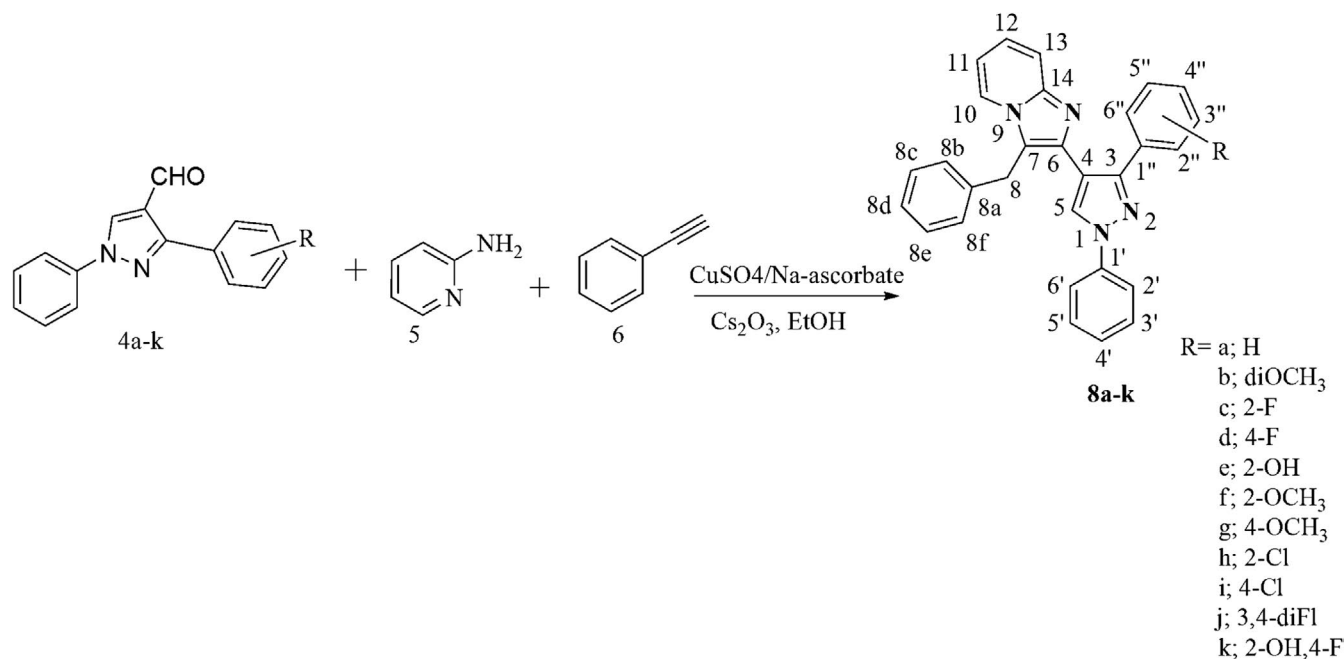
The synthetic route to the title compounds, 3-benzyl-2-(*N*-phenyl)-1-phenyl-1H-pyrazol-4-yl)imidazo[1,2- $\alpha$ ]pyridine (**8a-k**), is outlined in Scheme 1. The key starting materials, pyrazole aldehyde (**4a-k**), were synthesized by initial condensation of

phenyl hydrazine with acetophenones (**2a-k**), followed by Vilsmeier Haack formylation using a mixture of phosphorous oxychloride and dimethyl formamide. To monitor the reaction time and the amount of catalyst that will yield the desired product, pyrazole aldehyde (**4a**) was allowed to undergo one-pot, three-component reaction with 2-aminopyridine (**5**) and phenylacetylene (**6**) and catalysed by  $\text{CuSO}_4$ /sodium ascorbate under reflux in ethanol to furnish the pyrazole-imidazole compound **8a** in moderate yield, whilst the uncyclized propargyl amine **7a** as the main product. To improve the yield of the target compound, optimization studies were undertaken (Table 1). The amount of catalyst and temperature played a vital role in increasing the yield and decreasing the reaction time without forming the undesired side product. However,  $\text{CuSO}_4$  and glucose were found to be ineffective and the yield of desired product was not satisfactory which may be due to the bulkiness of the pyrazole aldehydes. The reaction proceeded well with 1:2  $\text{CuSO}_4$ /sodium ascorbate mixture affording the desired product pyrazole-imidazo[1,2- $\alpha$ ]pyridine hybrids **8a** (48%) along with **7a** (20%). An increase in  $\text{CuSO}_4$  (0.5) and NaAsc (1) produced 60% yield of pyrazole-imidazo[1,2- $\alpha$ ]pyridine. The yield increased when caesium carbonate ( $\text{Cs}_2\text{CO}_3$ ) was added at 100°C and was finally optimized to 70% with the same combination ( $\text{CuSO}_4$ :sodium ascorbate: $\text{Cs}_2\text{CO}_3$ ) in a ratio of 1:2:0.2 at 120°C for 12 hr. The side product was also absent under the same condition (Scheme 2).

**TABLE 1** Scope of various catalyst, reducing agent and temperature for the synthesis of pyrazole–imidazo[1,2- $\alpha$ ]pyridine scaffold

Entry	Solvent	Catalyst (mol%)	Temp (°C)	Time (hr)	Yield %
1	Ethanol	CuSO <sub>4</sub> ·H <sub>2</sub> O(1)/glucose(1)	80	12	trace
2	Ethanol	CuSO <sub>4</sub> ·H <sub>2</sub> O (1)/glucose(2)	100	24	35
3	Ethanol	CuSO <sub>4</sub> ·H <sub>2</sub> O (0.5)/NaAsc(1)	80	12	35
4	Ethanol	CuSO <sub>4</sub> ·H <sub>2</sub> O(0.5)/NaAsc(1)	100	24	48
5	Ethanol	CuSO <sub>4</sub> ·H <sub>2</sub> O(1)/NaAsc(2)	80	12	60
6	Ethanol	CuSO <sub>4</sub> ·H <sub>2</sub> O(1)/NaAsc(2)/Cs <sub>2</sub> CO <sub>3</sub> (0.2)	100	24	70
7	<b>Ethanol</b>	<b>CuSO<sub>4</sub>·H<sub>2</sub>O(1)/NaAsc(2)/Cs<sub>2</sub>CO<sub>3</sub>(0.2)</b>	<b>120</b>	<b>12</b>	<b>70</b>

Bold values indicates optimized condition employed for preparing the rest of the compounds (8a-k)

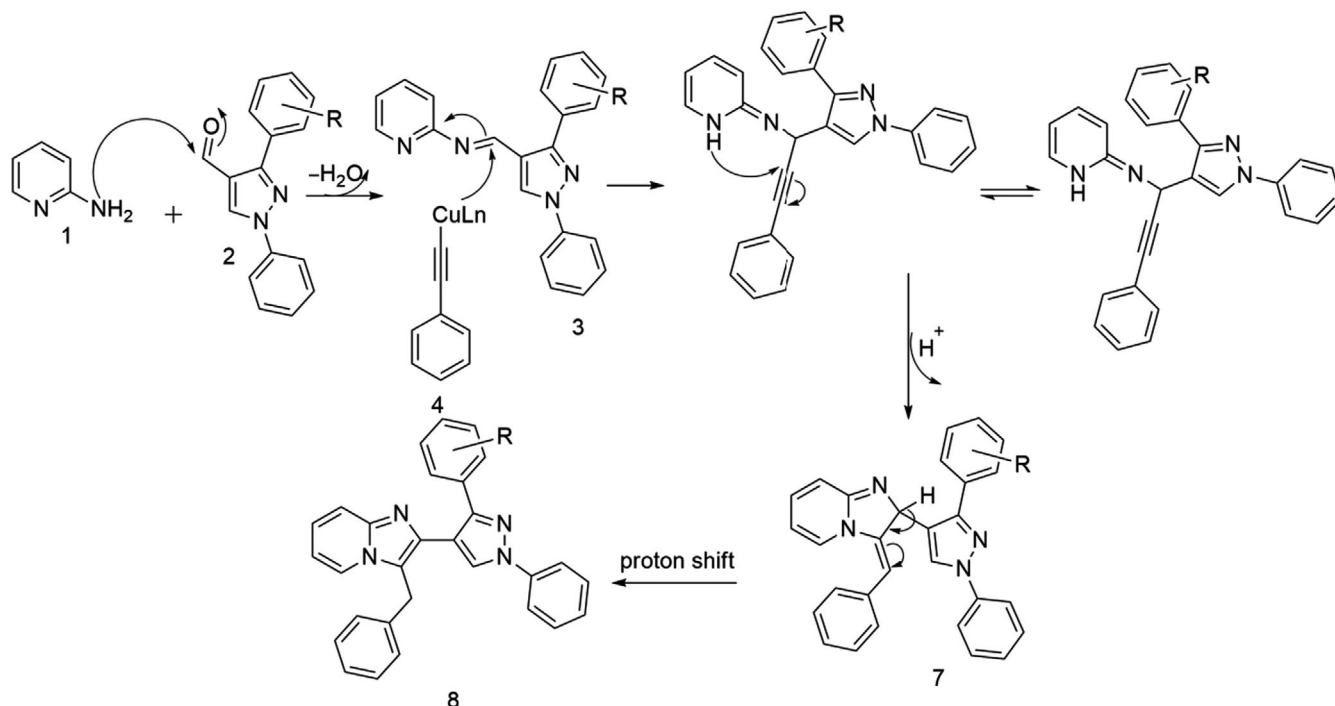
**SCHEME 2** Synthesis of pyrazole-imidazo[1,2- $\alpha$ ]pyridine derivatives

A plausible mechanism of reaction to rationalize the formation of pyrazole–imidazo[1,2- $\alpha$ ]pyridines is showed in Scheme 3. The domino reaction started with condensation between aminopyridine (**1**) and pyrazole aldehyde (**2**) followed by dehydration, which results in the formation of Schiff base (**3**). Cu (I), formed *via* sodium ascorbate-mediated reduction in Cu (II), inserts itself between carbon and hydrogen to form copper-acetylide complex (**4**), which subsequently attacks the iminic carbon to form intermediate (**5**), and this is followed by cyclization step initiated by an attack of on the alkyne unit by pyridine nitrogen to afford the target hybrids (**8**) (Scheme 3).

### 3.1 | Structural elucidation

The structures of the synthesised compounds were confirmed by their <sup>1</sup>H, <sup>13</sup>C and HRMS data. For example, **8b** showed a peak at *m/z* = 487.2142 [*M* + H]<sup>+</sup>, corresponding to the molecular formula C<sub>31</sub>H<sub>27</sub>N<sub>4</sub>O<sub>2</sub>. The <sup>1</sup>H NMR spectrum of compound **8b** showed a downfield H-5 singlet

resonance at 8.13 ppm, characteristic of the pyrazole ring proton. The upfield singlet resonance at 4.01 ppm was also characteristic of the benzylic methylene group. Two *3H* resonances for the methoxy groups could be seen at  $\delta$  3.83 (3''-OCH<sub>3</sub>) and 3.71 (4''-OCH<sub>3</sub>). The protons on the imidazopyridine ring, H-10 and H-12 overlapped at  $\delta$  7.66 and appears as a triplet with *J* = 6.8 Hz. In other compounds, H-10 is a clear doublet, for example in **8d**, where it appears at  $\delta$  7.61 (*J* = 9.1 Hz). However, H-12 always overlaps either with H-10 or with the aromatic protons and its true splitting pattern is not observed. The H-13 and H-11 resonances occur typically more upfield than H-10 and H-12 at  $\delta$  6.88, a doublet doublet (*J* = 7.8, 1.8 Hz) and a triplet at  $\delta$  6.68 (*J* = 7.8 Hz), respectively. The signals for the phenyl group attached to N-1 occurs as a typical doublet (H-2'/6') at  $\delta$  7.76 (*J* = 7.6 Hz) and two triplets at  $\delta$  7.45 and 7.28 attributed to H-3'/5' and H-4', respectively. The benzyl ring aromatic protons occur as a multiplet between  $\delta$  7.1 and 7.2. On the substituted aromatic ring at C-3 on the



**SCHEME 3** Plausible mechanism of reaction to formation of pyrazole Imidazo[1,2 $\alpha$ ]pyridines

**TABLE 2** Minimum bactericidal concentration (MBC) values of selected compounds ( $\mu\text{g/mL}$ )

Entry	Gram-positive		Gram-negative			
	MRSA ATCC BAA-1683	<i>S. aureus</i> ATCC 25,923	<i>E. coli</i> ATCC 8,739	<i>S. typhimurium</i> ATCC 25,922	<i>K. pneumoniae</i> ATCC 314,588	<i>P. aeruginosa</i> ATCC 27,853
<b>8b</b>	19.53	0.63	0.02	0.02	0.63	0.02
<b>8d</b>	2.50	0.63	0.63	0.63	0.63	0.63
<b>8e</b>	19.53	0.08	0.63	0.63	0.08	0.63
<b>8h</b>	19.53	0.63	0.02	0.02	0.02	0.08
<b>8i</b>	19.53	1.25	0.63	0.63	0.63	0.32
Ciprofloxacin	1.84	1.84	3.68	3.63	3.68	1.84

pyrazole moiety, H-2'' appears as a doublet at  $\delta$  7.35 with  $J = 1.2$  Hz, H-5'' as a doublet at  $\delta$  6.72 ( $J = 8.0$  Hz) and H-6'' overlaps with H-3'/5' at  $\delta$  7.45.

The  $^{13}\text{C}$  NMR spectrum showed the fully substituted carbon resonances of C-3, C-6, C-14, C-1' and C-7 as the most deshielded resonances at  $\delta$  151.4, 148.9, 144.8 and 139.9, respectively. Consequently, these carbon atoms are attached to nitrogen. The C-4 and C-8a resonances occurred more upfield at  $\delta$  115.1 and 118.7, respectively. The protonated carbons were assigned with the aid of the HSQC spectrum.

### 3.2 | Antibacterial activity

The synthesized pyrazole-imidazo[1,2- $\alpha$ ]pyridine conjugates were examined for their in vitro antibacterial activity

against two Gram-positive bacteria: methicillin-resistant *Staphylococcus aureus* and *Staphylococcus aureus*; and four Gram-negative bacteria: *Escherichia coli*, *Klebsiella pneumoniae*, *Pseudomonas aeruginosa* and *Salmonella typhimurium*. All selected compounds (zone of inhibition  $>9$  mm) showed excellent bactericidal activity against both Gram-positive and Gram-negative bacterial strains (Table 2). In most cases, except for MRSA, the activity of the compounds was better than that of the standard ciprofloxacin and recorded at  $<1$   $\mu\text{g/ml}$  for all strains (only **8i** was slightly above 1 at with MBC of 1.25  $\mu\text{g/ml}$  for *S. aureus*). Compound **8h** (2-Cl derivative) had excellent activity against Gram-negative strains with MBC  $<0.1$   $\mu\text{g/ml}$  for all Gram-negative strains, closely followed by **8b** (3,4-dimethoxy derivative) with MBC  $<0.1$   $\mu\text{g/ml}$  for three of the Gram-negative strains and 0.63  $\mu\text{g/ml}$  against *K. pneumoniae*. Note worthily, **8d** (4-F

Entry	MF	MW	nRB	nHB	nHD	TPSA	mlogP	Ro5
7a	C <sub>29</sub> H <sub>22</sub> N <sub>4</sub>	426.51	5	2	1	42.47	5.25	1
8a	C <sub>29</sub> H <sub>22</sub> N <sub>4</sub>	426.51	5	2	0	35.12	4.61	1
8b	C <sub>31</sub> H <sub>26</sub> N <sub>4</sub> O <sub>2</sub>	486.56	7	4	0	53.58	3.83	0
8c	C <sub>29</sub> H <sub>21</sub> FN <sub>4</sub>	444.50	5	3	0	35.12	4.97	1
8d	C <sub>29</sub> H <sub>21</sub> FN <sub>4</sub>	444.50	5	3	0	35.12	4.97	1
8e	C <sub>29</sub> H <sub>22</sub> N <sub>4</sub> O	442.51	5	3	0	35.12	4.05	0
8f	C <sub>30</sub> H <sub>24</sub> N <sub>4</sub> O	456.54	6	3	0	44.35	4.25	1
8g	C <sub>30</sub> H <sub>24</sub> N <sub>4</sub> O	456.54	6	3	0	44.35	4.24	1
8h	C <sub>29</sub> H <sub>21</sub> ClN <sub>4</sub>	460.96	5	2	0	35.12	5.07	1
8i	C <sub>29</sub> H <sub>21</sub> ClN <sub>4</sub>	460.96	5	2	0	35.12	5.07	1
8j	C <sub>29</sub> H <sub>20</sub> F <sub>2</sub> N <sub>4</sub>	462.49	5	4	0	35.12	7.56	1
8k	C <sub>29</sub> H <sub>20</sub> F <sub>2</sub> N <sub>4</sub>	460.50	5	4	1	55.35	4.41	1

Abbreviations: MF: molecular formula; mlogP: predicted octanol/water partition coefficient; MW: molecular weight; nRB: number of rotatable bond; nHBD: number of hydrogen bond donors; nHBA: number of hydrogen bond acceptors; Ro5: Lipinski violations; TPSA: topological polar surface area.

derivative) exhibited broad-spectrum antibacterial activity with MBC values <2.50 µg/ml against all bacterial strains; thus, a viable hit compound for broad-spectrum antibacterial agent development.

### 3.3 | Pharmacology

#### 3.3.1 | Lipinski's rule of five

SwissADME software was utilized to measure Lipinski's rule of five (Ro5) of the targeted compounds (Daina et al., 2017). The rule states that most molecules with good membrane permeability have not more than five hydrogen bond donors, not more than ten hydrogen bond acceptors, a polar surface area less than 140 Å, molecular weight not more than 500 g/mol and the calculated Log P (clogP) must be greater than 5 (or mlogP > 4.15). mlogP is the predicted octanol/water partition coefficient (Lipinski, Franco, Beryl, & Paul, 2012). SwissADME was also used to calculate topological polar surface area (TPSA), the surface belonging to polar atoms, a descriptor shown to correlate well with passive molecular transport through membranes, thus predicting transport properties of drugs (Ertl et al., 2000).

The calculated mlogP values and other pharmacokinetics properties that give insight into the absorption, distribution, metabolism, excretion and toxicity of the synthesized pyrazoles–imidazo[1,2- $\alpha$ ]pyridine analogues (8a–k) is shown in Table 3. The values of OH–NH polar fragments representing the proton donors and proton acceptors were between 0 and 4 for all synthesized compounds. The TPSA indicates that these compounds may have smooth and efficient binding to the receptor, high drug absorption and bio-availability, and they can be transported across blood–brain barriers (Beadle & Shoichet, 2002; Lipinski et al., 2012).

**TABLE 3** Physicochemical properties for pyrazole–imidazo[1,2- $\alpha$ ]pyridine scaffold compounds 7a and 8a–k predicted by SwissADME

Results of the calculations for the molecules designed in this study show that all molecules have potential for good in vivo absorption, since all the compounds show zero violation of the rule.

#### 3.3.2 | Molecular docking

In order to support our experimental antibacterial results, molecular studies were undertaken. All active compounds were docked into the binding site of enzyme glucosamine-6-phosphate, the enzyme responsible for the biosynthesis of peptidoglycan which occurs in the cytoplasmic membrane (Moraes et al., 2015). The purpose of docking simulations was to predict the ability of our compounds to bind in the active site of the enzyme and to explore their binding characteristics. Docking simulations were performed using autodock vina in PyRx0.8 with Auto-Grid options based on scoring functions (Trott & Olson, 2010). The results reveal that pyrazoles–imidazo[1,2- $\alpha$ ]pyridine hybrid show strong hydrogen bonding interaction with the amino acid residues of the protein.

The binding active sites and docked poses obtained were visualized with discovery studio visualize Figure 1. The computed binding energies indicated that all the active compounds formed stable complex with the enzyme. Compound 8h exhibited the strongest binding based on its lowest binding energy (–10.5 kcal/mol). The binding energies of 8b, 8d, 8e and 8i ranged between –9.5 and –10.0 kcal/mol also indicating their favourable binding with the receptor.

In order to get deeper insights into their host–guest relationship, the docked complexes were visualized using Discovery studio visualizer. Imidazole[1,2- $\alpha$ ]pyridine ring in 8b (methoxy at *meta* and *para* positions) formed an electrostatic potential ( $\pi$ -anion) with amino acids Glu24 and Arg21,

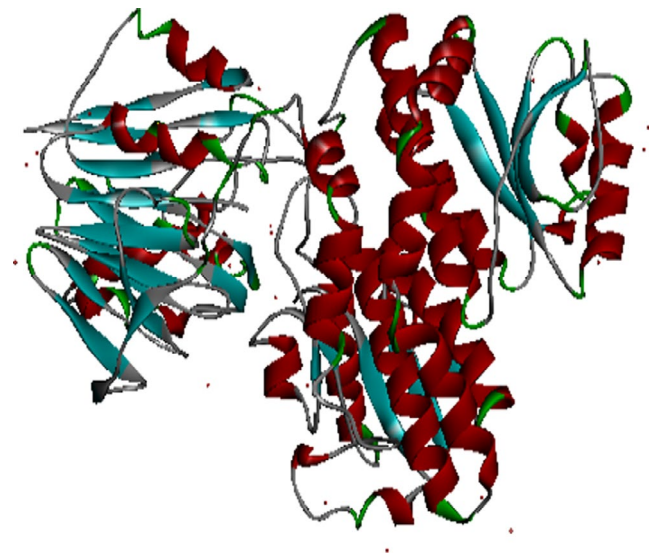


**FIGURE 1** Three-dimensional representation of glucosamine-6-phosphate synthase (PDB ID 1jxa)

and  $\pi$ - $\pi$  interactions between the phenyl group on the imidazole[1,2- $\alpha$ ]pyridine ring and the amino acid Tyr251. The phenyl group on the pyrazole moiety at the nitrogen increases the hydrophobic character of **8b** which formed  $\pi$ -alkyl and  $\pi$ - $\sigma$  interactions simultaneously with the amino acids Ile397 and Arg22 (Figure 2).

Compound **8d** (4-fluoro derivative) has a different conformation with respect to the other compounds (Figure 2). The fluorine at the *para* position forms a halogen bond with Arg22. The phenyl group also forms a hydrophobic interaction with Arg22 and Ile397. Two electrostatic interactions ( $\pi$ -anion and  $\pi$ -cation) occur with the pyrazole nucleus, and the unsubstituted phenyl moiety attached to the pyrazole nucleus by interacting with Glu24 and Lys50. A conventional hydrogen bond is seen between the nitrogen atoms of the imidazole[1,2- $\alpha$ ]pyridine moiety and hydroxyl group of Tyr251. A much lower number of hydrogen and  $\pi$ - $\pi$  interactions were formed.

Three amino acids Arg21, Arg22 and Gly24 located in the binding pocket played major roles in changing the conformation when bound to **8h** (Figure 2). The pyrazole nucleus and unsubstituted phenyl ring attached to the pyrazole nucleus form  $\pi$ -donor hydrogen bond interactions with Tyr251. One  $\pi$ -cation bond with bond length 3.31 Å was formed between Glu24 and imidazole[1,2- $\alpha$ ]pyridine moiety of **8h**.  $\pi$ -alkyl interactions are observed between pyrazole and imidazole[1,2- $\alpha$ ]pyridine moiety with Arg21, Arg22 and Ile397. The chlorine atom also formed hydrophobic interactions with Arg22.

Compound **8i** (4-Cl) also showed similar interactions as that of **8e** (2-OH). Both compounds formed hydrogen bonds with HOH709 through the imidazole nucleus, in addition to hydrophobic interactions with Arg21, Arg22, Ile397 and an electrostatic potential with Glu24 (Figure 2). The higher

number of hydrophobic interactions exhibited by these two compounds suggests their tighter fitting into the binding site of GlcN-6-P synthase and accounts for their high activity (**BE 8i** & **8e** = -10.0 kcal/mol).

It can be concluded that the docked compounds probably show their antibacterial activity by inhibiting the glucosamine-6-phosphate synthase enzyme, an important enzyme for the formation of bacterial cell wall.

#### General procedure for the synthesis of 1-phenyl-2-(phenylethylidene)hydrazine (**3a-k**)

Acetophenones (**2**) were added to phenylhydrazine (**1**) (100.0 mg, 1.51 mmol) dissolved in ethanol, with stirring and allowed to heat for 1 hr at 70°C. A precipitate was formed upon cooling, collected by filtration and recrystallized from ethanol at room temperature to produce the corresponding imines in yields of 90%.

#### General procedure for the synthesis of 1,3-diphenyl-1H-pyrazole-4-carbaldehydes (**4a-k**)

The imines **3a-k** (12 mmol) was added to a cold solution of dimethylformamide (40.0 mmol, 30 ml) in phosphorylchloride (40.0 mmol, 6.30 ml), and the mixture stirred at 60°C for 6 hr. The product was then poured onto ice-crushed and neutralized with 10% NaHCO<sub>3</sub>. The precipitate that formed was filtered, washed with water and allowed to dry to produce the pyrazole carbaldehydes with yield between 90% and 95%.

#### General procedure for the synthesis of pyrazole-imidazo[1,2- $\alpha$ ]pyridine (**8a-k**)

A mixture of 2-aminopyridine (2.0 mmol, 0.188 g) and substituted pyrazole aldehydes (1.0 mmol, 0.233 g) was dissolved in 10 ml ethanol. Phenylacetylene (1.0 mmol), CuSO<sub>4</sub> (20 mol%), sodium ascorbate (40 mol%) and caesium carbonate (0.5 mmol, 0.2 g) were then added successively to the reaction mixture, and the contents refluxed for 12 hr and monitored by TLC to completion. The reaction mixture was concentrated under reduced pressure and purified using silica gel column chromatography (EtOAc 6:4 Hex) to produce the product **8a-k**.

#### 3-Benzyl-2-(1,3-diphenyl-1H-pyrazol-4-yl)imidazo[1,2- $\alpha$ ]pyridine **8a**

Yellow oil; Yield: 65%; IR  $\nu_{\max}$  3,056, 2,925, 2,853, 1,942, 1,597, 1,495 cm<sup>-1</sup>;  $\delta$  8.29 (1H, s, H-5), 7.73 (3H, d,  $J$  = 8.0 Hz, H-2'/6', 10), 7.60 (3H, m, H-3''/5'', 12), 7.37 (2H, t,  $J$  = 8.0 Hz, H-3'/5'), 7.21 (5H, m, H-2''/6'', 4', 8d, 8c/8e), 7.06 (3H, m, H-8b/8f, 4''), 6.77 (1H, d,  $J$  = 8.0 Hz, H-13), 6.69 (1H, t,  $J$  = 4.0 Hz, H-11), 3.84 (2H, s, H-8), <sup>13</sup>C NMR (100 MHz, CDCl<sub>3</sub>):  $\delta$  151.3 (C-3), 143.6 (C-6), 139.8 (C-14), 136.0 (C-1'), 134.6 (C-7), 133.1 (C-1''), 129.4 (C-3'/5'), 129.3 (C-5), 128.8 (C-8b/8f), 128.5 (8c/8e), 128.1 (C-4''), 127.9

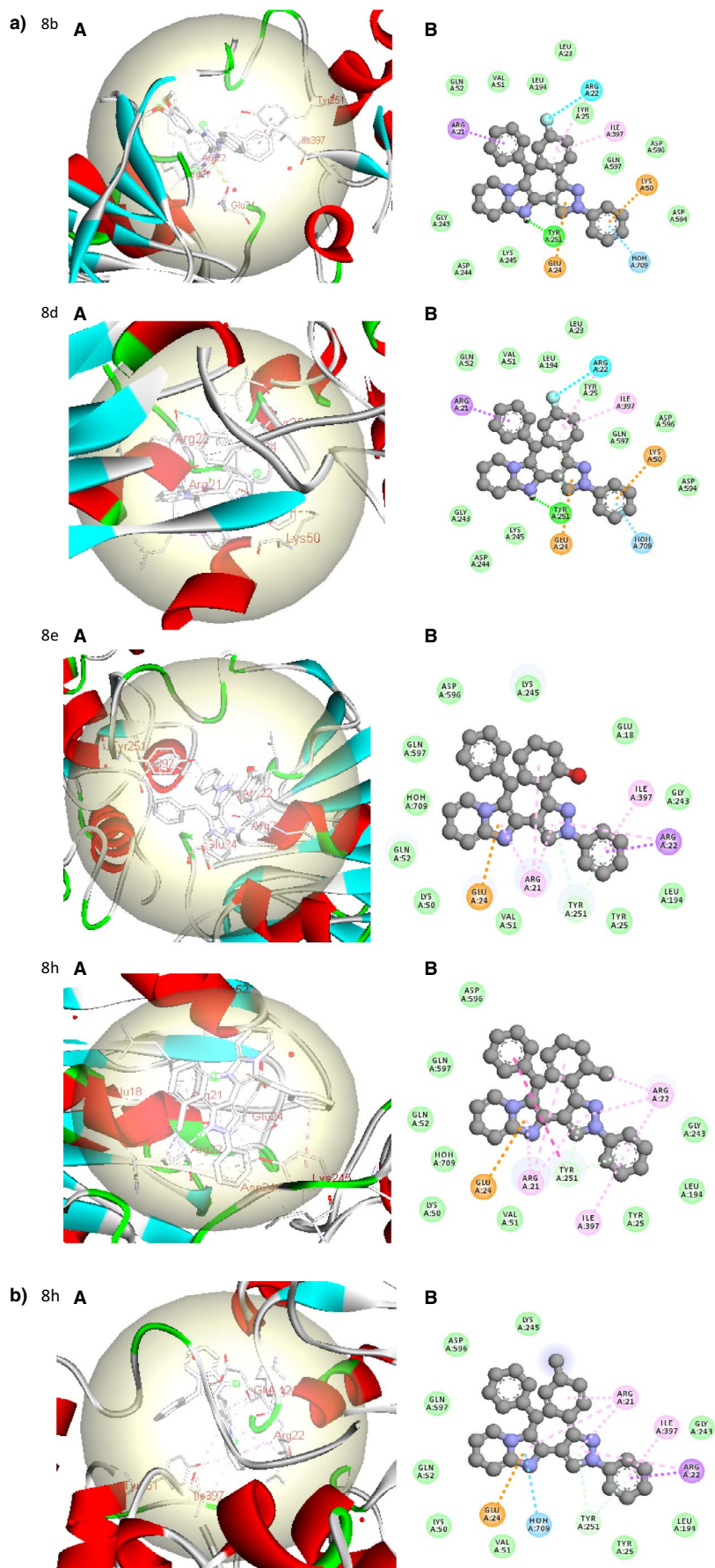


**FIGURE 2** Docked complex of pyrazole-imidazole of compound **8b**, **8d**, **8e**, **8h** and **8i** with GlcN-6-P synthase (PDB code: 1jxa). (a) Binding sphere is shown as light yellow with interacting amino acids of the protein. (b) 2D molecular docking showing hydrogen bond, electrostatic and hydrophobic interactions. ■ H<sub>2</sub>O-bond, ■  $\pi$ -anion, ■  $\pi$ -donor hydrogen bond, ■  $\pi$ - $\sigma$  bond, ■  $\pi$ - $\pi$  T shaped, ■  $\pi$ -alkyl

(3"/16"), 127.8 (C-2"/16"), 126.9 (C-12), 126.7 (C-4'), 125.8 (C-8d), 123.9 (C-10), 119.9 (C-8a), 119.2 (C-2'/6'), 116.6 (C-11), 113.5 (C-4), 113.2 (C-13), 29.4 (C-8); HRMS (pos) [ $M + H$ ] 427.1923 [calcd for  $C_{29}H_{22}N_4$  427.1923].

*3-Benzyl-2-(3-(3,4-dimethoxyphenyl)-1-phenyl-1H-pyrazol-4-yl)imidazo[1,2- $\alpha$ ]pyridine***8b**

Yellow oil; Yield: 66%; IR  $\nu_{\max}$  3,287, 3,112, 2,925, 2,853, 2,033, 1,598, 1,774, 1,671  $\text{cm}^{-1}$ ;  $^1\text{H}$  NMR (400 MHz,  $\text{CDCl}_3$ ):  $\delta$  8.12 (1H, s, H-5), 7.76 (2H, d,  $J = 7.6$  Hz, H-2'/6'), 7.66 (2H, t,  $J = 6.8$  Hz, H-12/10), 7.45 (3H, t,  $J = 7.6$  Hz, H-3'/5',6"), 7.35 (1H, d,  $J = 1.2$  Hz, H-2"), 7.28 (1H, t,  $J = 7.6$  Hz, H-4'), 7.20 (5H, m, H-8d, 8c/8e, 8b/8f), 6.88 (1H, dd,  $J = 7.8, 1.8$  Hz, H-13), 6.72 (1H, d,  $J = 8.0$  Hz, H-5"), 6.68 (1H, t,  $J = 7.8$  Hz, H-11), 3.71 (3H, s, H-4a), 4.01 (2H, s, H-8), 3.82 (3H, s, H-3a);  $^{13}\text{C}$  NMR (100 MHz,  $\text{CDCl}_3$ ):  $\delta$  151.4 (C-3), 148.9 (C-6), 144.8 (C-14), 144.8 (C-1'), 139.9 (C-7), 136.7 (C-1a), 129.4 (C-5/3'/5'), 128.7 (C-8b/8f), 127.8 (C-8c/8e), 126.7 (C-12), 126.5 (C-4'), 126.1 (C-1"), 124.1 (C-8d), 123.6 (C-10), 120.5 (C-6"), 119.1 (C-2'/6'), 118.7 (C-8a), 117.4 (C-11), 115.1 (C-4), 112.2 (C-13), 111.2 (C-2"), 111.0 (C-5"), 55.8 (C-3a), 55.7 (C-4a), 29.6 (C-8); HRMS (pos) [ $M + H$ ] 487.2142 [calcd for  $C_{31}H_{27}N_4O_2$  487.2134].

*3-Benzyl-2-(3-(2-fluorophenyl)-1-phenyl-1H-pyrazol-4-yl)imidazo[1,2- $\alpha$ ]pyridine***8c**

Brown oil; Yield: 65%; IR  $\nu_{\max}$  3,649, 3,024, 2,548, 1,929, 1,794, 1,596, 1,494  $\text{cm}^{-1}$ ;  $^1\text{H}$  NMR (400 MHz,  $\text{CDCl}_3$ ):  $\delta$  8.18 (1H, s, H-5), 7.70 (2H, d,  $J = 7.9$  Hz, H-2'/6'), 7.51 (3H, m, H-10,3",12), 7.36 (2H, t,  $J = 7.9$  Hz, H-3'/5'), 7.22 (1H, t,  $J = 7.9$  Hz, H-4'), 6.95–7.15 (6H, m, H-5"/8b/8f/8c/8e/8d), 6.87 (1H, t,  $J = 8.2$  Hz, H-4"), 6.76–6.80 (2H, m, H-6"/13), 6.56 (1H, t,  $J = 7.8$  Hz, H-11), 3.95 (2H, s, H-8);  $^{13}\text{C}$  NMR (400 MHz,  $\text{CDCl}_3$ ):  $\delta$  161.4 (d,  $J = 248.6$  Hz, C-2"), 158.9 (C-3), 147.0 (C-6), 144.8 (C-14), 139.9 (C-1'), 136.4 (C-7), 131.6 (d,  $J = 3.0$  Hz, C-6"), 129.9 (d,  $J = 7.8$  Hz, C-4"), 129.5 (C-3'/5'), 128.7 (C-8b/8f), 128.0 (C-5), 127.7 (C-8c/8e), 126.7 (C-12), 126.6 (C-4'), 124.1 (C-5"), 124.0 (C-8d), 123.6 (C-10), 121.5 (d,  $J = 14.5$  Hz, C-1"), 119.2 (C-2'/6'), 118.8 (C-8a), 117.3 (C-11), 117.3 (C-4), 115.9 (d,  $J = 21.6$  Hz, C-3"), 112.0 (C-13), 29.4 (C-8); HRMS (pos) [ $M + H$ ] 445.1831 [calcd for  $C_{29}H_{21}FN_4$ , 445.1829].

*3-Benzyl-2-(3-(4-fluorophenyl)-1-phenyl-1H-pyrazol-4-yl)imidazo[1,2- $\alpha$ ]pyridine***8d**

Dark brown oil; Yield: 62%; IR  $\nu_{\max}$  3,024, 2,925, 1,929, 1,794, 1,596, 1,494;  $^1\text{H}$  NMR (400 MHz,  $\text{CDCl}_3$ ):  $\delta$  8.32 (1H, s, H-5), 7.79 (2H, d,  $J = 7.9$  Hz, H-2'/6'), 7.61 (1H, d,  $J = 9.1$  Hz, H-10), 7.40–7.51 (5H, m, H-3'/5', 2"/6", 12), 7.29 (1H, t,  $J = 7.0$  Hz, H-4'), 7.09–7.14 (7H, m, H-3"/5", 8b/8f, 8c/8e, 8d), 6.75–6.78 (1H, m, H-13), 6.62 (1H, t,  $J = 6.7$  Hz, H-11), 3.95 (2H, s, H-8);  $^{13}\text{C}$  NMR (100 MHz,  $\text{CDCl}_3$ ):  $\delta$  149.6 (C-3), 145.0 (C-6), 139.8 (C-14), 136.4 (C-1'), 136.2

(C-7), 135.0 (C-1"), 129.5 (d,  $J = 8.2$  Hz, C-2"/6"), 129.5 (C-5/3'/5'), 128.8 (C-8b/8f), 127.9 (d,  $J = 18.5$  Hz, C-3'/5"), 127.7 (C-8c/8e), 126.7 (C-12), 126.0 (C-4'), 124.3 (C-8d), 123.7 (C-10), 119.7 (C-8a), 119.1 (C-2'/6'), 117.5 (C-11), 115.4 (C-4) 112.3 (C-13), 29.6 (C-8); HRMS (pos) [ $M + H$ ] 445.1833 [calcd for  $C_{29}H_{22}FN_4$ , 445.1829].

*3-Benzyl-2-(3-(2-hydroxyphenyl)-1-phenyl-1H-pyrazol-4-yl)imidazo[1,2- $\alpha$ ]pyridine***8e**

Yellowish solid powder; mp 163–165°C; Yield: 68%; IR  $\nu_{\max}$  3,050, 2,924, 2,854, 2,531, 1,941, 1,688, 1,597, 1,493;  $^1\text{H}$  NMR (400 MHz,  $\text{CDCl}_3$ ):  $\delta$  8.31 (1H, s, H-5), 7.99 (2H, d,  $J = 4.6$  Hz, H-2a), 7.78 (2H, d,  $J = 7.6$  Hz, H-2'/6'), 7.58 (1H, d,  $J = 9.0$  Hz, H-10), 7.42–7.51 (4H, m, H-3', 3", 5', 12), 7.27 (1H, t,  $J = 7.4$  Hz, H-4'), 7.18 (1H, td,  $J = 7.6, 1.6$  Hz, H-8d), 7.08–7.13 (5H, m, H-4", 8b, 8f, 8c, 8e), 6.75–6.78 (2H, m, H-13,5"), 6.60 (1H, t,  $J = 0.7$  Hz, H-11), 6.47 (1H, d,  $J = 8.2$  Hz, H-6"), 3.95 (2H, s, H-8);  $^{13}\text{C}$  NMR (100 MHz,  $\text{CDCl}_3$ ):  $\delta$  156.1 (C-2"), 150.1 (C-3), 144.8 (C-6), 139.1 (C-14), 139.1 (C-1'), 136.5 (C-7), 129.7 (C-5), 129.6 (C-3'/5'), 128.9 (C-8b/8f), 128.6 (C-8c/8e), 127.8 (C-4"/6"), 127.0 (C-12), 126.9 (C-4'), 124.5 (C-8d), 123.7 (C-10), 120.1 (C-8a), 119.4 (C-5"), 119.0 (C-2'/6'), 118.1 (C-1"), 117.9 (C-11), 117.6 (C-3"), 115.2 (C-4), 112.5 (C-13), 29.7 (C-8); HRMS (pos) [ $M + H$ ] 443.1875 [calcd for  $C_{29}H_{23}N_4O$  443.1872].

*3-Benzyl-2-(3-(2-methoxyphenyl)-1-phenyl-1H-pyrazol-4-yl)imidazo[1,2- $\alpha$ ]pyridine***8f**

Brownish solid powder; mp 158–160°C; Yield: 68%; IR  $\nu_{\max}$  3,362, 3,052, 2,923, 2,852, 1,941, 1,658, 1,598, 1,494;  $^1\text{H}$  NMR (400 MHz,  $\text{CDCl}_3$ ):  $\delta$  8.31 (1H, s, H-5), 7.78 (1H, d,  $J = 8.0$  Hz, H-2'/6'), 7.61 (1H, d,  $J = 8.9$  Hz, H-10), 7.52 (1H, d,  $J = 6.8$  Hz, H-6"), 7.45 (2H, t,  $J = 8.4$  Hz, H-3'/5'), 7.42 (1H, d,  $J = 8.0$  Hz, H-12), 7.27 (1H, d,  $J = 7.4$  Hz, H-8d), 7.21 (1H, t,  $J = 8.5$  Hz, H-4'), 7.10 (4H, m, H-8b/8f,8c/8e), 6.90 (1H, t,  $J = 7.4$  Hz, H-4"), 6.76–6.78 (2H, m, H-13,5"), 6.65 (1H, d,  $J = 8.3$  Hz, H-3"), 6.61 (1H, t,  $J = 6.7$  Hz, H-11), 3.92 (2H, s, H-8), 3.37 (3H, s, H-2a);  $^{13}\text{C}$  NMR (100 MHz,  $\text{CDCl}_3$ ):  $\delta$  157.4 (C-2"), 149.4 (C-3), 144.4 (C-6), 137.4 (C-14), 140.1 (C-1'), 136.6 (C-7), 131.6 (C-6"), 129.7 (C-5), 129.4 (C-3'/5'), 128.6 (C-8b/8f), 127.7 (C-4"), 127.7 (C-8c/8e), 126.4 (C-12), 126.4 (C-4'), 123.8 (C-8d), 123.5 (C-5"), 122.8 (C-1"), 120.7 (C-10), 119.2 (C-2'/6'), 118.6 (C-8a), 117.2 (C-11), 112.3 (C-4), 111.9 (C-3"), 111.3 (C-13), 55.3 (C-2a), 29.2 (C-8); HRMS (pos) [ $M + H$ ] 457.2041 [calcd for  $C_{30}H_{25}N_4O$ , 457.2028].

*3-benzyl-2-(3-(4-methoxyphenyl)-1-phenyl-1H-pyrazol-4-yl)imidazo[1,2- $\alpha$ ]pyridine***8g**

Brown oil; Yield: 70%; IR  $\nu_{\max}$  3,361, 3,058, 2,924, 2,548, 1,679, 1,597, 1,495  $\text{cm}^{-1}$ ;  $^1\text{H}$  NMR (400 MHz,  $\text{CDCl}_3$ ):  $\delta$  8.20 (1H, s, H-5), 7.81 (3H, d,  $J = 8.7$  Hz, H-2'/6',10), 7.67–7.70 (1H, m, H-12), 7.64 (d,  $J = 8.8$  Hz, H-2"/6"), 7.47 (2H, t,

$J = 7.5$  Hz, H-3'/5'), 7.27–7.31 (2H, m, H-8c/8e), 7.15–7.20 (4H, m, H-4', 8b/8f, 8d), 6.90–6.92 (2H, m, H-13), 6.63 (2H, d,  $J = 8.8$  Hz, H-3''/5''), 6.71 (1H, t,  $J = 7.2$  Hz, H-11), 4.02 (2H, s, H-8), 3.79 (3H, s, H-4a);  $^{13}\text{C}$  NMR (400 MHz,  $\text{CDCl}_3$ ):  $\delta_{\text{C}}$  159.5 (C-4''), 151.2 (C-3), 144.9 (C-6), 140.0 (C-14), 136.8 (C-1'), 136.7 (C-7), 129.4 (C-5,3'/5'), 129.1 (C-8b/8f), 128.7 (C-8c/8e), 127.8 (C-2''/6''), 126.6 (C-12), 126.4 (C-4'), 126.0 (C-1''), 124.0 (C-8d), 123.6 (C-10), 119.7 (C-8a), 119.0 (C-2'/6'), 117.5 (C-11), 115.0 (C-4), 113.8 (3''/5''), 112.1 (C-13), 55.2 (C-4a), 29.6 (C-8); HRMS (pos) [ $M + H$ ] 457.2025 [calcd for  $\text{C}_{30}\text{H}_{25}\text{N}_4\text{O}$ , 457.2028].

### 3-Benzyl-2-(3-(2-chlorophenyl)-1-phenyl-1H-pyrazol-4-yl)imidazo[1,2- $\alpha$ ]pyridine**8h**

Brown solid powder; mp 159–161°C; Yield: 65%; IR  $\nu_{\text{max}}$  3,056, 2,925, 2,855, 1,942, 1,715, 1,633, 1,597  $\text{cm}^{-1}$ ;  $^1\text{H}$  NMR (400 MHz,  $\text{CDCl}_3$ ):  $\delta$  8.27 (1H, s, H-5), 7.75 (1H, d,  $J = 9.0$  Hz, H-2'/6'), 7.60–7.62 (1H, m, H-3''), 7.55 (1H, d,  $J = 9.0$  Hz, H-10'), 7.32–7.48 (5H, m, H-3'/5,4'',5'',12), 7.23 (1H, t,  $J = 7.3$  Hz, H-4'), 7.15 (1H, dt,  $J = 7.7, 1.6$  Hz, H-8d), 7.05–7.09 (4H, m, H-8b/8f,8c/8e), 6.73–6.74 (1H, m, H-13), 6.56 (1H, t,  $J = 8.0$  Hz, H-11), 6.41 (1H, d,  $J = 8.0$  Hz, H-6''), 3.92 (2H, s, H-8);  $^{13}\text{C}$  NMR (100 MHz,  $\text{CDCl}_3$ ):  $\delta_{\text{C}}$  149.6 (C-3), 145.0 (C-6), 139.9 (C-14), 136.7 (C-7), 133.8 (C-1'), 132.8 (C-1''), 132.3 (C-2''), 132.2 (C-3''), 129.8 (4''), 129.3 (C-3'/5',5), 128.6 (C-8b/8f), 127.8 (C-5''), 127.6 (C-8c/8e), 126.7 (C-12), 126.6 (C-4'), 126.4 (C-6''), 123.9 (C-8d), 123.7 (C-10), 119.2 (C-2'/6'), 118.7 (C-8a), 117.7 (C-4), 117.3 (C-11), 111.9 (C-13), 29.2 (C-8); HRMS (pos) [ $M + H$ ] 461.1531 [calcd for  $\text{C}_{29}\text{H}_{22}\text{N}_4\text{Cl}$ , 461.1533].

### 3-Benzyl-2-(3-(4-chlorophenyl)-1-phenyl-1H-pyrazol-4-yl)imidazo[1,2- $\alpha$ ]pyridine**8i**

Yellow oil; Yield: 62%; IR  $\nu_{\text{max}}$  3,485, 3,057, 2,925, 2,854, 1,941, 1,717, 1,597, 1,494  $\text{cm}^{-1}$ ;  $^1\text{H}$  NMR (400 MHz,  $\text{CDCl}_3$ ):  $\delta$  8.08 (1H, s, H-5), 7.71 (1H, d,  $J = 9.3$  Hz, H-10), 7.69 (1H,  $J = 7.8$  Hz, H-2'/6'), 7.59 (2H, d,  $J = 8.4$  Hz, H-2''/6''), 7.35–7.50 (5H, m, H-3'/5',3''/5'',12), 7.21 (1H, t,  $J = 7.8$  Hz, H-4'), 7.03–7.13 (5H, m, H-8d,8c/8e,8b/8f), 6.83 (1H, d,  $J = 7.6$  Hz, H-13), 6.63 (1H, t,  $J = 7.8$  Hz, H-11), 3.97 (2H, s, C-8),  $^{13}\text{C}$  NMR (100 MHz,  $\text{CDCl}_3$ ):  $\delta_{\text{C}}$  149.6 (C-3), 144.9 (C-6), 139.9 (C-14), 136.5 (C-1'), 136.1 (C-7), 133.8 (C-1''), 132.2 (C-2''/6''), 129.8 (C-3''/5''), 129.5 (C-5, 3'/5'), 128.7 (C-8b/8f), 127.6 (8c/8e), 126.7 (C-12), 126.6 (C-4'), 124.1 (C-8d), 123.7 (C-10), 119.2 (C-2'/6'), 119.0 (C-8a), 117.5 (C-4), 117.2 (C-11), 112.0 (C-13), 29.2 (C-8); HRMS (pos) [ $M + H$ ] 461.1535 [calcd for  $\text{C}_{29}\text{H}_{22}\text{ClN}_4$ , 461.1533].

### 3-Benzyl-2-(3-(3,4-difluorophenyl)-1-phenyl-1H-pyrazol-4-yl)imidazo[1,2- $\alpha$ ]pyridine**8j**

Yellow oil; Yield: 68%; IR  $\nu_{\text{max}}$  3,271, 3,057, 2,924, 2,854, 1,952, 1,672, 1,598, 1,496  $\text{cm}^{-1}$ ;  $^1\text{H}$  NMR (400 MHz,  $\text{CDCl}_3$ ):  $\delta$  8.09 (1H, s, H-5), 7.73 (2H, d,  $J = 8.0$  Hz, H-2'/6'),

7.68 (1H, d,  $J = 7.0$  Hz, H-10), 7.58 (1H, ddd,  $J = 9.8, 7.9, 1.9$  Hz, H-5''), 7.40–7.47 (3H, m, H-3'/5'/12), 7.30 (1H, t,  $J = 7.4$  Hz, H-4'), 7.16–7.19 (4H, m, H-8c/8e, 8b/8f), 7.01 (1H, t,  $J = 8.4$  Hz, H-8d), 6.91 (1H, dd,  $J = 8.0, 1.4$  Hz, H-13), 6.72 (1H, t,  $J = 6.8$  Hz, H-11), 6.56–6.62 (1H, m, H-2''), 4.07 (2H, s, H-8),  $^{13}\text{C}$  NMR (100 MHz,  $\text{CDCl}_3$ ):  $\delta_{\text{C}}$  151.3 (C-3), 149.0 (C-6), 139.7 (C-14), 136.4 (C-1'), 136.1 (C-7), 130.3 (C-1''), 129.5 (C-5,3'/5'), 128.9 (C-8b/8f), 127.6 (8c/8e), 126.8 (C-12/4'), 124.4 (C-8d), 124.1 (dd,  $J = 6.2, 3.6$  Hz, C-6''), 123.6 (C-10), 119.8 (C-8a), 119.9 (C-2'/6'), 117.6 (C-11), 117.1 (d,  $J = 17.1$  Hz, C-2''), 116.9 (d,  $J = 18.4$  Hz, C-5''), 115.2 (C-4), 112.4 (C-13), 29.5 (C-8); HRMS (pos) [ $M + H$ ] 463.1730 [calcd for  $\text{C}_{29}\text{H}_{21}\text{F}_2\text{N}_4$ , 463.1734].

### 3-Benzyl-2-(3-(4-fluoro-2-hydroxyphenyl)-1-phenyl-1H-pyrazol-4-yl)imidazo[1,2- $\alpha$ ]pyridine**8k**

White solid powder; mp 146–148°C; Yield: 68%; IR  $\nu_{\text{max}}$  3,071, 2,925, 2,854, 1,733, 1,671, 1,596, 1,493  $\text{cm}^{-1}$ ;  $^1\text{H}$  NMR (400 MHz,  $\text{CDCl}_3$ ):  $\delta$  8.04 (1H, s, H-5), 7.78 (1H, dd,  $J = 6.7$  Hz, 10), 7.64–7.69 (3H, m, H-2'/6'/6''), 7.39–7.48 (3H, m, H-3'/4'/5'/12), 7.30–7.34 (1H, m, H-8d), 7.22–7.26 (4H, m, H-8b/8f, 8c/8e), 6.99 (1H, d,  $J = 4.0$  Hz, H-3''), 6.98–7.00 (1H, m, H-3''), 6.75–6.78 (2H, m, H-13,5''), 6.43 (1H, t,  $J = 7.0$  Hz, H-11), 4.20 (2H, s, H-8a),  $^{13}\text{C}$  NMR (100 MHz,  $\text{CDCl}_3$ ):  $\delta_{\text{C}}$  163.5 (d,  $J = 245.4$  Hz, C-4''), 158.0 (d,  $J = 12.6$ , C-2''), 149.6 (C-3), 144.9 (C-6), 139.0 (C-14), 136.4 (C-7), 135.9 (C-1''), 130.0 (d,  $J = 10.2$  Hz, C-6''), 129.7 (C-5,3'/5'), 129.0 (C-8b/8f), 127.8 (8c/8e), 127.1 (C-12), 127.0 (C-4'), 124.7 (C-8d), 123.7 (C-10), 112.0 (C-8a), 119.0 (C-2'/6'), 117.5 (C-11), 114.9 (C-1''), 114.7 (C-4), 112.7 (C-13), 106.7 (d,  $J = 21.7$  Hz, C-5''), 105.0 (d,  $J = 23.4$  Hz, C-3''), 29.6 (C-8); HRMS (pos) [ $M + H$ ] 461.1771 [calcd for  $\text{C}_{29}\text{H}_{22}\text{FN}_4\text{O}$ , 461.1778].

## 4 | CONCLUSION

The antibacterial potential of the newly synthesized 3-benzyl-2-(*N*-phenyl)-1-phenyl-1H-pyrazol-4-yl)imidazo[1,2- $\alpha$ ]pyridine derivatives was analysed against two Gram-positive bacteria (methicillin-resistant *S. aureus* and *S. aureus*) and four Gram-positive bacteria (*E. coli*, *S. typhimurium*, *K. pneumonia* and *P. aeruginosa*). Compounds (**8b**, **8d**, **8e**, **8i**, **8h**) demonstrated excellent bactericidal activities, even better than ciprofloxacin. The most resistant bacterial species for these compounds were *E. coli*, *S. typhimurium*, *K. pneumonia* and *P. aeruginosa*. Molecular docking of these active compounds into the binding sites of GlcN-6-P synthase further verified their differential binding affinities for the target proteins as well druglikeness. The biological and in silico investigations of the newly synthesized hybrids proffer their viability as novel antibacterial

agents, with the potential ability to reduce virulence and pathogenicity of drug-resistant bacteria in vivo.

## ACKNOWLEDGMENTS

NK thanks the National Research Foundation South Africa for a Competitive Grant for Rated Researchers (Grant No. 118534) and Incentive Funding for Rated Researchers (Grant No. 114817). We would also like to thank the Centre for High Performance Computing based in Cape Town for access to computational resources.

## CONFLICT OF INTEREST

The authors declare no conflict of interest.

## DATA AVAILABILITY STATEMENT

The data that support the findings of this study are available on request from the corresponding author.

## ORCID

Oluwakemi Ebenezer  <https://orcid.org/0000-0003-1054-9665>

## REFERENCES

- Al-Tel, T. H., & Al-Qawasmeh, R. A. (2010). Post Groebke-Blackburn multicomponent protocol: Synthesis of new polyfunctional imidazo [1, 2-a] pyridine and imidazo [1, 2-a] pyrimidine derivatives as potential antimicrobial agents. *European Journal of Medicinal Chemistry*, *45*, 5848–5855. <https://doi.org/10.1016/j.ejmech.2010.09.049>
- Bagdi, A. K., Sougata, S., Kamarul, M., & Alakananda, H. (2015). Synthesis of imidazo [1, 2-a] pyridines: A decade update. *Chemical Communications*, *51*, 1555–1575. <https://doi.org/10.1039/C4CC08495K>
- Barreateau, H., Andreja, K., Audrey, B., Matej, S., Stanislav, G., & Didier, B. (2008). Cytoplasmic steps of peptidoglycan biosynthesis. *FEMS Microbiology Reviews*, *32*, 168–207. <https://doi.org/10.1111/j.1574-6976.2008.00104.x>
- Beadle, B. M., & Shoichet, B. K. (2002). Structural basis for imipenem inhibition of class C  $\beta$ -lactamases. *Antimicrobial Agents and Chemotherapy*, *46*, 3978–3980. <https://doi.org/10.1128/AAC.46.12.3978-3980.2002>
- Chmara, H., & Borowski, E. (1986). Bacteriolytic effect of cessation of glucosamine supply, induced by specific inhibition of glucosamine-6-phosphate synthetase. *Acta Microbiologica Polonica*, *35*, 15–27.
- Daina, A., Olivier, M., & Vincent, Z. (2017). SwissADME: A free web tool to evaluate pharmacokinetics, drug-likeness and medicinal chemistry friendliness of small molecules. *Scientific Reports*, *7*, 42717. <https://doi.org/10.1038/srep42717>
- Ebrahimipour, S. Y., Iran, S., Jim, S., Hadi, E., Michal, D., Nima, K., & Vaclav, E. (2016). Antimicrobial activity of aroylhydrazone-based oxido vanadium (v) complexes: In vitro and in silico studies. *New Journal of Chemistry*, *40*, 2401–2412. <https://doi.org/10.1039/C5NJ02594J>
- Ebrahimipour, S., Mehrji, K., Jonathan, W., & Sahar, F. (2018). Preparation, crystal structure, spectroscopic studies, DFT calculations, antibacterial activities and molecular docking of a tridentate Schiff base ligand and its cis-MoO<sub>2</sub> complex. *Applied Organometallic Chemistry*, *32*, e4233. <https://doi.org/10.1002/aoc.4233>
- Ertl, P., Bernhard, R., & Paul, S. (2000). Fast calculation of molecular polar surface area as a sum of fragment-based contributions and its application to the prediction of drug transport properties. *Journal of Medicinal Chemistry*, *43*, 3714–3717. <https://doi.org/10.1021/jm000942e>
- Finn, J., Karen, M., Mike, M., Siya, R., Yingfei, Y., Ximao, W., ... Dennis, K. (2003). Discovery of a potent and selective series of pyrazole bacterial methionyl-tRNA synthetase inhibitors. *Bioorganic & Medicinal Chemistry Letters*, *13*, 2231–2234. [https://doi.org/10.1016/S0960-894X\(03\)00298-1](https://doi.org/10.1016/S0960-894X(03)00298-1)
- Guchhait, S. K., Ajay, L. C., & Garima, P. (2012). CuSO<sub>4</sub>-glucose for in situ generation of controlled Cu (I)-Cu (II) bicatalysts: Multicomponent reaction of heterocyclic azine and aldehyde with alkyne, and cycloisomerization toward synthesis of N-fused imidazoles. *Journal of Organic Chemistry*, *77*, 4438–4444. <https://doi.org/10.1021/jo3003024>
- Gueiffier, C., & Gueiffier, A. (2007). Recent progress in the pharmacology of imidazo [1, 2-a]pyridines. *Mini Reviews in Medicinal Chemistry*, *7*, 888–899. <https://doi.org/10.2174/138955707781662645>
- Hayakawa, M., Ken-ichi, K., Hiroyuki, K., Tomonobu, K., Takahide, O., Mayumi, Y., ... Florence, I. R. (2007). Synthesis and biological evaluation of sulfonylhydrazone-substituted imidazo [1, 2-a] pyridines as novel PI3 kinase p110 $\alpha$  inhibitors. *Bioorganic & Medicinal Chemistry*, *15*, 5837–5844. <https://doi.org/10.1016/j.bmc.2007.05.070>
- Hiremathad, A., Mahadeo, R. P., Chethana, K. R., Karam, C., Amelia, S., & Rangappa, S. K. (2015). Benzofuran: An emerging scaffold for antimicrobial agents. *RSC Advances*, *5*, 96809–96828. <https://doi.org/10.1016/j.bmc.2007.05.070>
- Jayanna, N. D., Vagdevi, H. M., Dharshan, J. C., Raghavendra, R., & Sandeep, B. T. (2013). Synthesis, antimicrobial, analgesic activity, and molecular docking studies of novel 1-(5, 7-dichloro-1, 3-benzoxazol-2-yl)-3-phenyl-1H-pyrazole-4-carbaldehyde derivatives. *Medicinal Chemistry Research*, *22*, 5814–5822. <https://doi.org/10.1007/s00044-013-0565-9>
- Khan, S. A., Abdullah, M. A., Rahman, R. M., Shaaban, A. E., Faisal, A., Mohmmad, Y. W., & Kamlesh, S. (2017). Multistep synthesis of fluorine-substituted pyrazolopyrimidine derivatives with higher antibacterial efficacy based on in vitro molecular docking and density functional theory. *Journal of Heterocyclic Chemistry*, *54*, 3099–3107. <https://doi.org/10.1002/jhet.2923>
- Kumara, H. K., Suhas, R., Suyoga, V., Shobha, M., & Channe, G. D. (2018). A correlation study of biological activity and molecular docking of Asp and Glu linked bis-hydrazones of quinazolinones. *RSC Advances*, *8*, 10644–10653. <https://doi.org/10.1039/C8RA00531A>
- Lipinski, C. A., Franco, L., Beryl, W. D., & Paul, J. F. (2012). Experimental and computational approaches to estimate solubility and permeability in drug discovery and development settings. *Advanced Drug Delivery Reviews*, *64*, 4–17. [https://doi.org/10.1016/S0169-409X\(00\)00129-0](https://doi.org/10.1016/S0169-409X(00)00129-0)

- Márquez-Flores, Y. K., Campos-Aldrete, M. E., Salgado-Zamora, H., Correa-Basurto, J., & Meléndez-Camargo, M. E. (2012). Docking simulations, synthesis, and anti-inflammatory activity evaluation of 2-(N-alkyl) amino-3-nitroimidazo [1, 2-a] pyridines. *Medicinal Chemistry Research*, *21*, 775–782. <https://doi.org/10.1007/s00044-011-9585-5>
- Milewski, S. (2002). Glucosamine-6-phosphate synthase—the multifacets enzyme. *Biochimica Et Biophysica Acta (BBA) - Protein Structure and Molecular Enzymology*, *1597*, 173–192. [https://doi.org/10.1016/S0167-4838\(02\)00318-7](https://doi.org/10.1016/S0167-4838(02)00318-7)
- Montero-Morán, G. M., Lara-González, S., Alvarez-Añorve, L. I., Plumbridge, J. A., & Calcagno, M. L. (2001). On the multiple functional roles of the active site histidine in catalysis and allosteric regulation of *Escherichia coli* glucosamine 6-phosphate deaminase. *Biochemistry*, *40*, 10187–10196. <https://doi.org/10.1021/bi0105835>
- Moraes, G. L., Guelber, C. G., Paulo, R. M., Cláudio, N. A., Thavendran, G., Hendrik, G. K., ... Jerônimo, L. (2015). Structural and functional features of enzymes of *Mycobacterium tuberculosis* peptidoglycan biosynthesis as targets for drug development. *Tuberculosis (Edinb)*, *95*, 95–111. <https://doi.org/10.1016/j.tube.2015.01.006>
- Palanisamy, P., Samsom, J. J., Packianathan, T. M., & Sudalaiandi, K. (2013). Synthesis, characterization, antimicrobial, anticancer, and antituberculosis activity of some new pyrazole, isoxazole, pyrimidine and benzodiazepine derivatives containing thiochromeno and benzothiepine moieties. *RSC Advances*, *3*, 19300–19310. <https://doi.org/10.1039/C3RA42283F>
- Pandit, S. S., Mahesh, R. K., Yashwant, B. P., Nitin, P. L., & Vijay, M. K. (2018). Synthesis and in vitro evaluations of 6-(hetero)-aryl-imidazo [1, 2-b] pyridazine-3-sulfonamide's as an inhibitor of TNF- $\alpha$  production. *Bioorganic & Medicinal Chemistry Letters*, *28*, 24–30. <https://doi.org/10.1016/j.bmcl.2017.11.026>
- Pannu, N., & Nadim, M. K. (2008). An overview of drug-induced acute kidney injury. *Critical Care Medicine*, *36*, S216–S223. <https://doi.org/10.1097/CCM.0b013e318168e375>
- Rao, R. N., Barnali, M., Ranjit, T., & Kaushik, C. (2018). Efficient access to imidazo [1, 2-a] pyridines/pyrazines/pyrimidines via catalyst-free annulation reaction under microwave irradiation in green solvent. *ACS Combinatorial Science*, *20*, 164–171. <https://doi.org/10.1021/acscombsci.7b00173>
- Sarojini, B. K., Krishna, B. G., Darshanraj, C. G., Bharath, B. R., & Manjunatha, H. (2010). Synthesis, characterization, in vitro and molecular docking studies of new 2, 5-dichloro thienyl substituted thiazole derivatives for antimicrobial properties. *European Journal of Medicinal Chemistry*, *45*, 3490–3496. <https://doi.org/10.1016/j.ejmech.2010.03.039>
- Tomi, I. H. R., Al-Daraji, A.-H.-R., Abdula, A., & Al Marjani, M. F. (2016). Synthesis, antimicrobial and docking study of three novel 2, 4, 5-triarylimidazole derivatives. *Journal of Saudi Chemical Society*, *20*, S509–S516. <https://doi.org/10.1016/j.jscs.2013.03.004>
- Trott, O., & Olson, A. J. (2010). AutoDock Vina: Improving the speed and accuracy of docking with a new scoring function, efficient optimization, and multithreading. *Journal of Computational Chemistry*, *31*, 455–461. <https://doi.org/10.1002/jcc.21334>
- Tsuiki, S., & Miyagi, T. (1977). Neoplastic alterations of glucosamine 6-phosphate synthase in rat liver. *Advances in Enzyme Regulation*, *15*, 35–52. [https://doi.org/10.1016/0065-2571\(77\)90008-5](https://doi.org/10.1016/0065-2571(77)90008-5)
- Xi, J.-B., Yan-Fen, F., Brendan, F., Meng-Li, Z., Tong, Z., Yan-Nan, K., ... Hong-Yu, L. (2017). Structure-based design and synthesis of imidazo [1, 2-a] pyridine derivatives as novel and potent Nek2 inhibitors with in vitro and in vivo antitumor activities. *European Journal of Medicinal Chemistry*, *126*, 1083–1106. <https://doi.org/10.1016/j.ejmech.2016.12.026>
- Yang, Y., Yuan, Z., Ling, Y. Y., Leilei, Z., Lianghui, S. I., Huibin, Z., ... Jinpei, Z. (2017). Discovery of imidazopyridine derivatives as novel c-Met kinase inhibitors: Synthesis, SAR study, and biological activity. *Bioorganic Chemistry*, *70*, 126–132. <https://doi.org/10.1016/j.bioorg.2016.12.002>

## SUPPORTING INFORMATION

Additional supporting information may be found online in the Supporting Information section.

**How to cite this article:** Ebenezer O, Awolade P, Koorbanally N, Singh P. New library of pyrazole–imidazo[1,2- $\alpha$ ]pyridine molecular conjugates: Synthesis, antibacterial activity and molecular docking studies. *Chem Biol Drug Des*. 2019;00:1–12. <https://doi.org/10.1111/cbdd.13632>